Supplementary Material

Atazanavir inhibits SARS-CoV-2 replication and pro-inflammatory cytokine production

Natalia Fintelman-Rodrigues[1,9#], Carolina Q. Sacramento[1,9#], Carlyle Ribeiro Lima[9,#], Franklin Souza da Silva[2,9], André C. Ferreira[1,3,9], Mayara Mattos[1,9], Caroline S. de Freitas[1,9], Vinicius Cardoso Soares[1], Suelen da Silva Gomes Dias[1], Jairo R. Temerozo[4,5], Milene D. Miranda[6], Aline R. Matos[6], Fernando A. Bozza[7,8], Nicolas Carels[9], Carlos Roberto Alves[2], Marilda M. Siqueira[6], Patrícia T. Bozza[1], Thiago Moreno L. Souza[1,9,*]

# - These authors contributed equally to this work

1 – Laboratório de Imunofarmacologia, Instituto Oswaldo Cruz (IOC), Fundação Oswaldo Cruz (Fiocruz), Rio de Janeiro, RJ, Brazil.

2 – Laboratório de Biologia Molecular e Doenças Endêmicas, IOC, Fiocruz, Rio de Janeiro, RJ, Brazil.

3 – Universidade Iguaçu, Nova Iguaçu, RJ, Brazil.

4 – Laboratório de Pesquisas sobre o Timo, IOC, Fiocruz, Rio de Janeiro, RJ, Brazil.

5 - National Institute for Science and Technology on Neuroimmunomodulation (INCT/NIM), IOC, Fiocruz, Rio de Janeiro, RJ, Brazil.

6 – Laboratório de Vírus Respiratório e do Sarampo, IOC, Fiocruz, Rio de Janeiro, RJ, Brazil.

7 – Instituto Nacional de Infectologia Evandro Chagas, Fiocruz, Rio de Janeiro, RJ, Brazil

8 – Instituto D'or de Pesquisa e Ensino, Rio de Janeiro, RJ, Brazil

9 - National Institute for Science and Technology on Innovation in Diseases of Neglected Populations (INCT/IDPN), Center for Technological Development in Health (CDTS), Fiocruz, Rio de Janeiro, RJ, Brazil.

***Correspondence footnote:**

Thiago Moreno L. Souza, PhD

****

Fundação Oswaldo Cruz

Centro de Desenvolvimento Tecnológico em Saúde (CDTS)

Instituto Oswaldo Cruz (IOC)

Pavilhão Osório de Almeida, sala 16

Av. Brasil 4365, Manguinhos, Rio de Janeiro - RJ, Brasil, CEP 21060340

Tel.: +55 21 2562-1311

Email: tmoreno@cdts.fiocruz.br

Additional Results *in silico*

Molecular Dynamics

The enzyme-LPV complex was stable with a RMSD value not exceeding 3 Å, but when considering LPV alone, its RMSD exceeded 4 Å over the entire simulation (Figure S1A). By contrast, when complexed with ATV, the RMSD of SCV2-MP reached as much as 4 Å in the last 20 ns of the simulation, while the RMSD of ATV alone did not exceed 3 Å over the 100 ns (Figure S1B). After the step of energy minimization, at the beginning of the molecular dynamics, LPV presented 4 hydrogen bonds with the amino acids Thr25, Ser46, Gly143, and Gln189 (Figures S2A and S3A). After 100 ns of molecular dynamics, LPV interacted with Ser46 HIS41 (Figures 3A and 4A).

ATV's interaction, after energy minimization, occurred with residue Gln189 (Figure S2B and S3B), but after 100 ns of molecular dynamics, Glu166 acted as a hydrogen acceptor and His164 as a hydrogen donor (Figure 3B and 4B).

Tables

Table S1. Interactions from Atanazavir (ATV) with the residues from the active site.

Docking Interactions of ATA		
Ligand	Residues	Distance, Å
ATV:H32	ASN142:OD1	1.91
ATV:H32	HIS164:O	2.64
ATV:H8	GLU166:OE1	2.44

Table S2. Interactions from Lopinavir (LPV) with the residues from the active site before (*) and after MD.

Molecular Dynamics Interactions of LPV		
Ligand	Residues	Distance, Å
LPV:O1	THR25:HG1	1.99*
LPV:O2	SER45:HG	1.75*
LPV:O	GLY143:H	2.31*
LPV:O2	GLN189:HE21	1.95*
LPV:O2	SER46:HD	1.70
LPV:O1	HIS41:HE2	2.03

Table S3. Interactions from Atanazavir (ATV) with residues from the active site before (*) and after MD.

Molecular Dynamics Interactions of ATV		
Ligand	Residues	Distance, Å
ATV:H28	GLN189:OE1	2.04*
ATV:H31	HIE167:O	1.87
ATV:H2	GLU166:O	2.51

Legend for the Figures

Figure S1. A representative structure of Mpro (PDB:6LU7) was color coded to show the electrostatic potential of residues in the active site for negative (blue) and positive (red) charges. Panel A, the cavities of ligand interaction designated S1*, S1 and S2 in the absence of inhibitors. Panel B, placement of LPV (cyan) docked in the S1* and S2 regions of the active site. Panel C, placement of ATV (orange) docked in the S1* and S1 regions of the active site.

Figure S2. Two-dimensional (2D) representations of the interactions of LPV (A) and ATV (B) in the Mpro active site based on a molecular docking analysis. Two hydrogen bonds are predicted between ATV and Mpro.

Figure S3. Root Mean Square Deviation (RMSD) along 100 ns of MD simulation of the Mpro (black) when complexed with A) LPV (red) and B) ATV(red). (A) LPV (red) is rather unstable while Mpro (black) remains stable. In (B), it is Mpro (black) that is destabilized while ATV (red) remains stable along the MD simulation.

Figure S4. Representative images of the Root Mean Square Deviation (RMSD) along 100 ns of molecular dynamics (MD) simulation. LPV (A) and ATV (B) are positioned in the Mpro active site at the beginning of 100 ns simulation.

Figure S5. Two-dimensional (2D) representation of the interactions of LPV (A) and ATV (B) into Mpro's active site at the beginning of 100 ns RMSD.

107

108

109

110

111

112

113

114

115

116

117

118

119

120

121

122

123

124

125

126

127

128

129

Figure S1

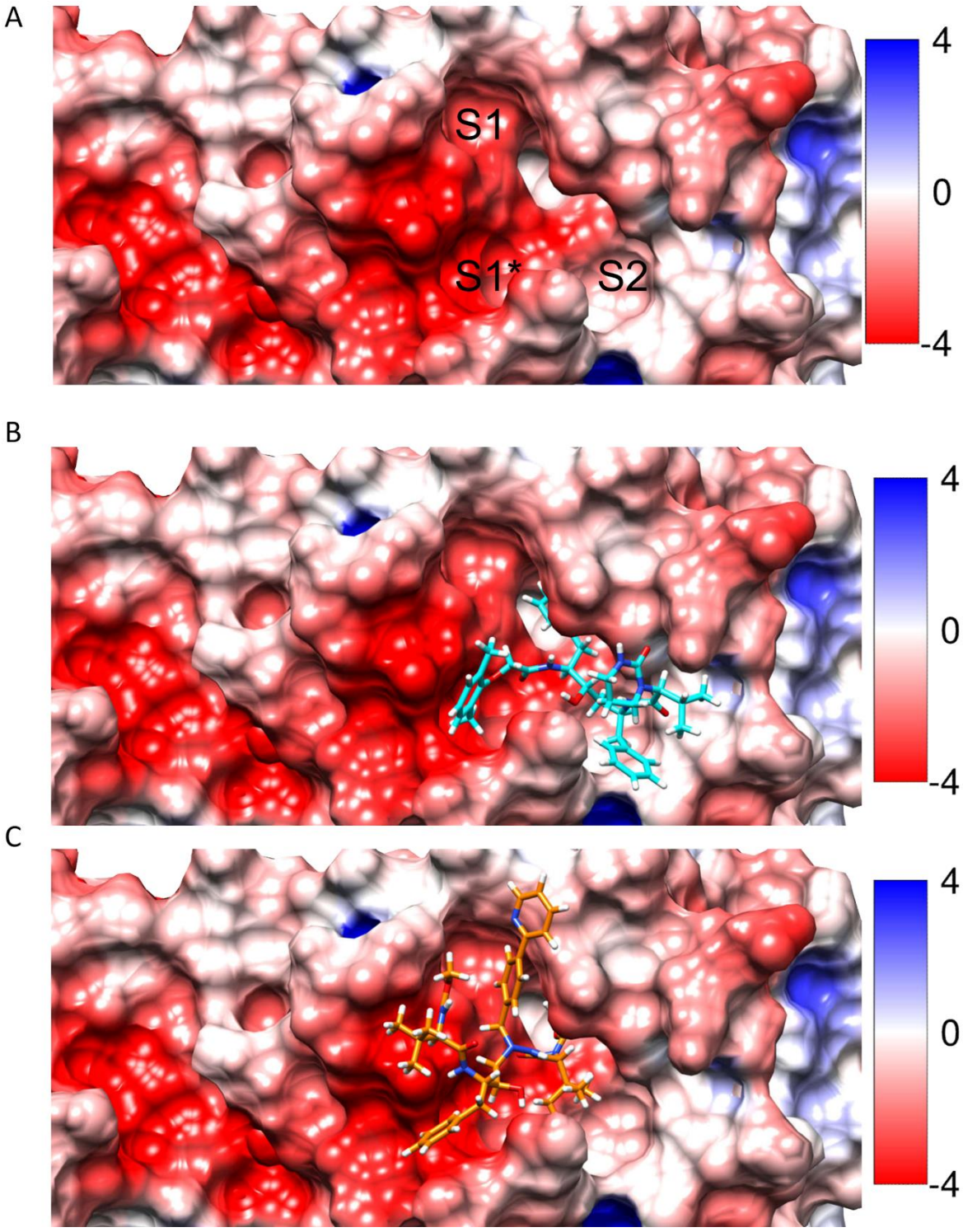

Figure S2

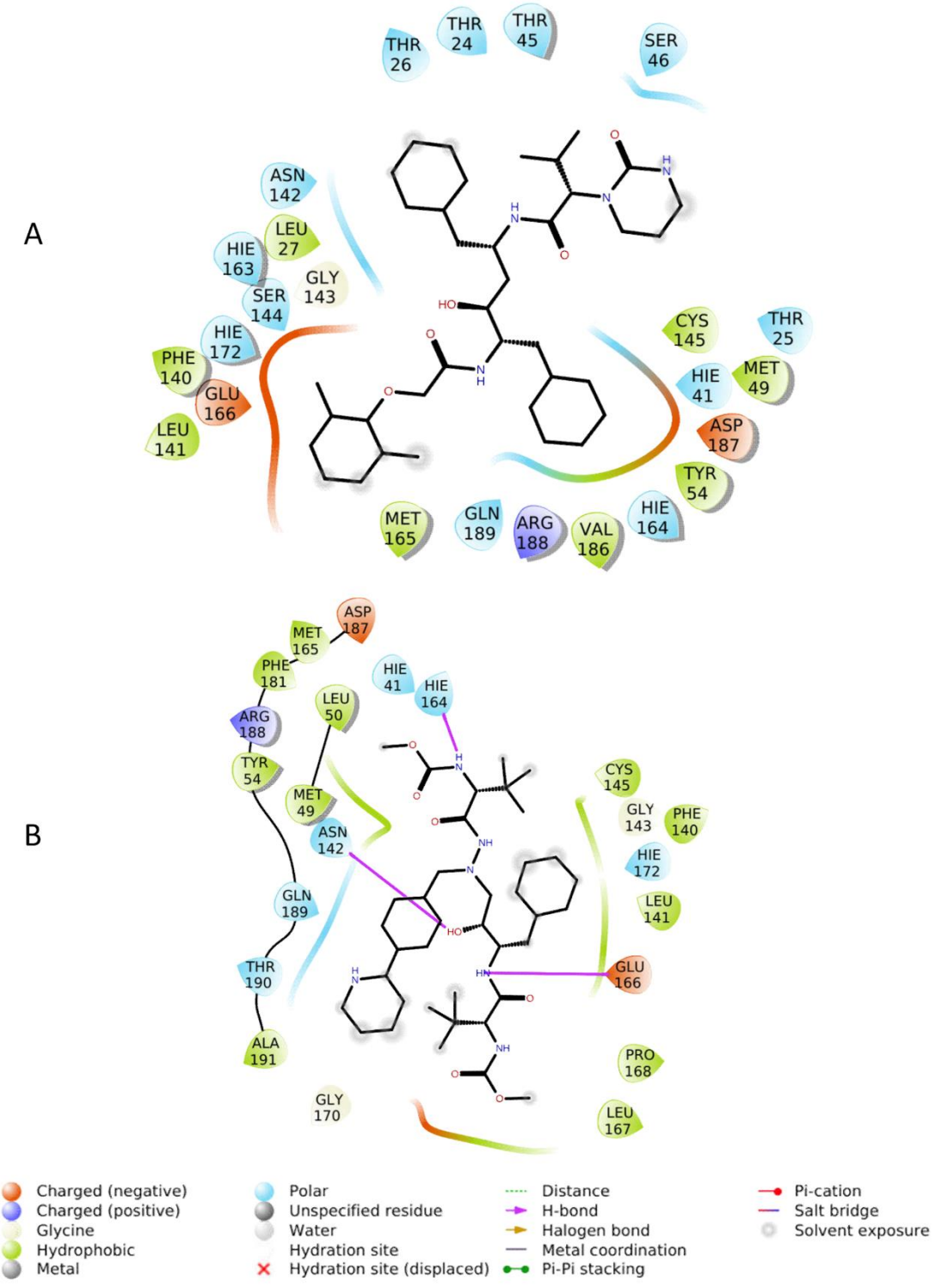
A
THR 26
THR 24
THR 45
SER 46
ASN 142
LEU 27
HIE 163
GLY 143
SER 144
HIE 172
PHE 140
GLU 166
LEU 141
CYS 145
THR 25
HIE 41
MET 49
ASP 187
TYR 54
MET 165
GLN 189
ARG 188
VAL 186
HIE 164
B
ASP 187
MET 165
PHE 181
HIE 41
HIE 164
LEU 50
ARG 188
TYR 54
MET 49
ASN 142
GLN 189
THR 190
ALA 191
GLY 170
CYS 145
GLY 143
PHE 140
HIE 172
LEU 141
GLU 166
PRO 168
LEU 167
Charged (negative)
Charged (positive)
Glycine
Hydrophobic
Metal
Polar
Unspecified residue
Water
Hydration site
Hydration site (displaced)
Distance
H-bond
Halogen bond
Metal coordination
Pi-Pi stacking
Pi-cation
Salt bridge
Solvent exposure

136

137 Figure S3

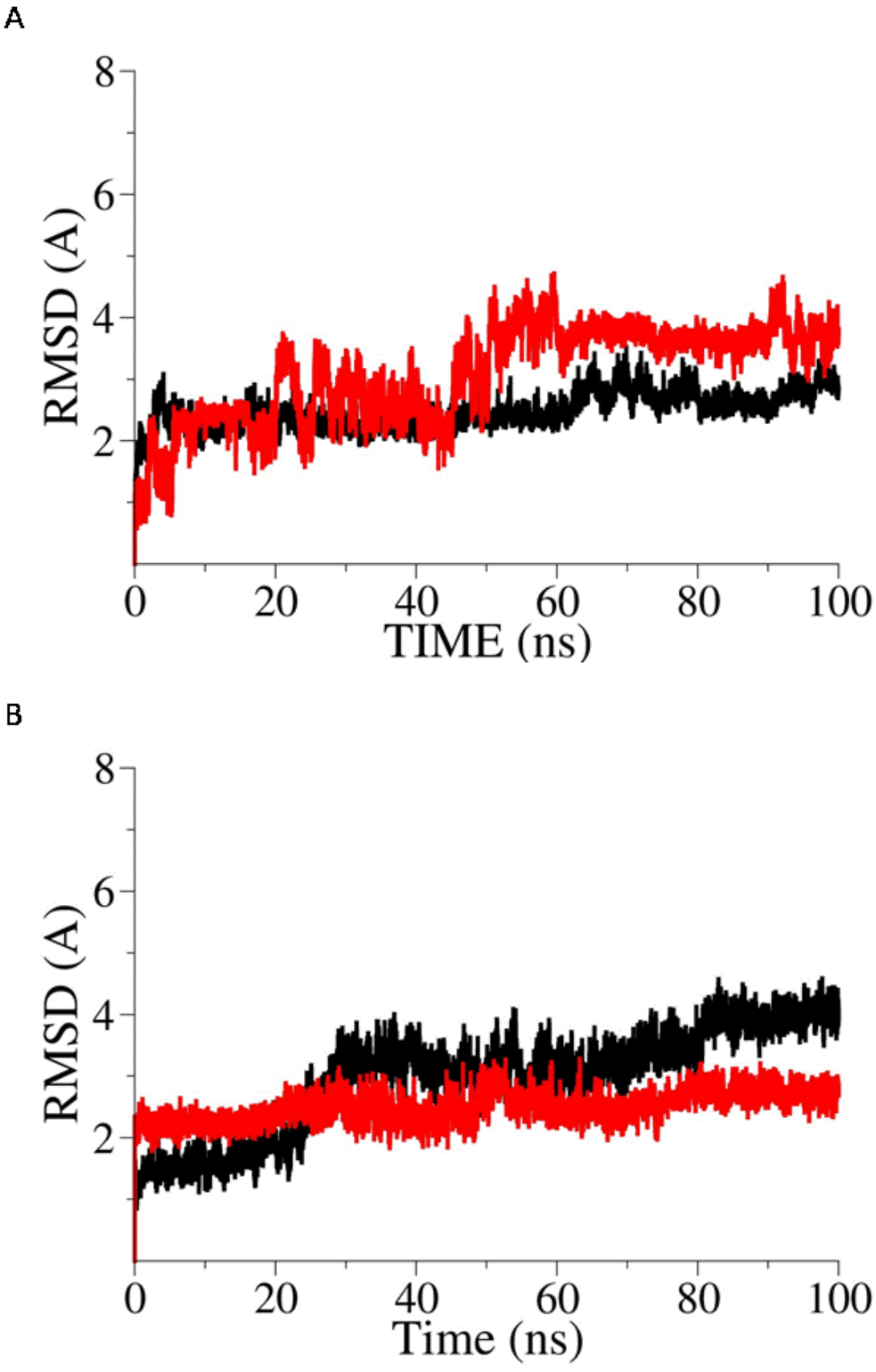

138

Figure S4

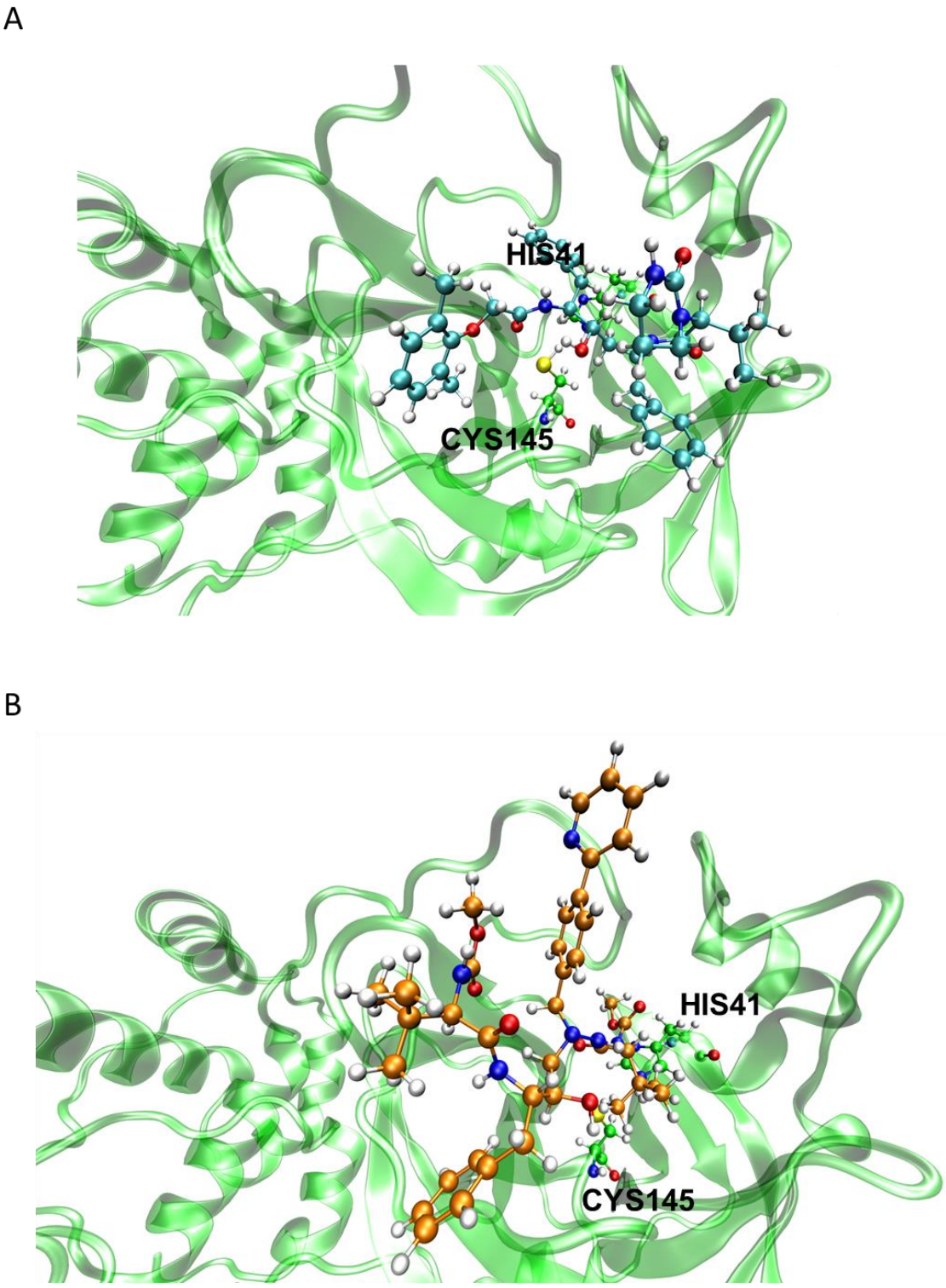

142 Figure S5

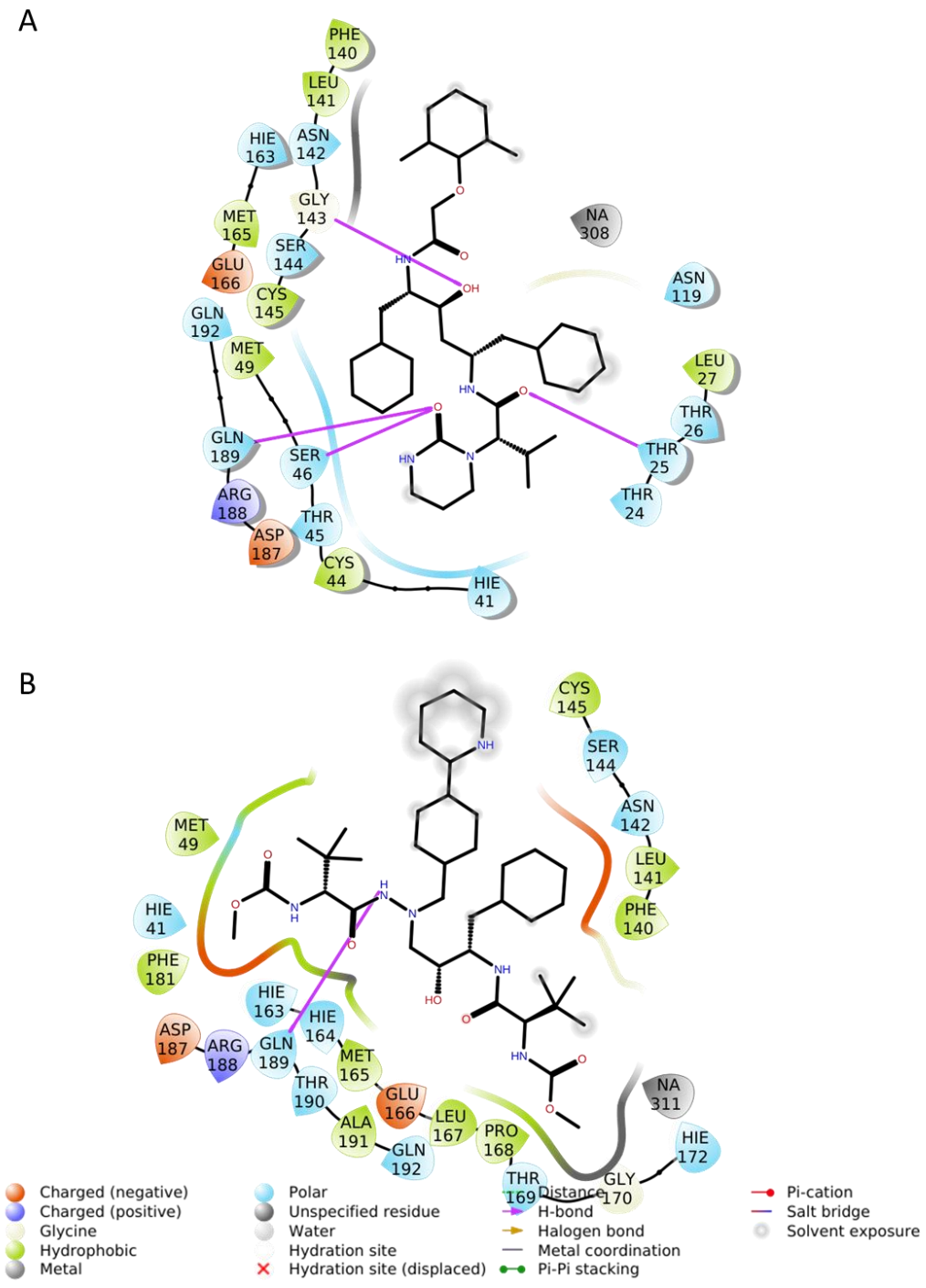

143